Noise-induced transition of atoms between dynamic phase-space attractors in a parametrically excited atomic trap

Kihwan Kim,[1,*] Myoung-Sun Heo,[1] Ki-Hwan Lee,[1] Hyoun-Jee Ha,[1] Kiyoub Jang,[1] Heung-Ryoul Noh,[2] and Wonho Jhe[1,†]
[1]*School of Physics and Center for Near-field Atom-photon Technology, Seoul National University, Seoul 151-747, Korea*
[2]*Department of Physics, Chonnam National University, Gwangju 500-757, Korea*
(Received 2 March 2005; published 4 November 2005)

We have investigated the noise-induced transition of cold atoms between double or triple phase-space attractors that are produced in the parametrically driven magneto-optical trap. The transition rates between two dynamic attractors, directly measured for various modulation frequencies and amplitudes, are in good agreement with calculations from the dynamic version of Kramers' theory and Monte Carlo simulations. For the triple attractors, the transition rates are measured indirectly through the steady-state population and the results are also in agreement with simulations. Our experiment may be useful for study of nonlinear dynamic problems involving transitions between states far from equilibrium.

DOI: 10.1103/PhysRevA.72.053402 PACS number(s): 32.80.Pj, 05.45.−a

There have been many studies on the fluctuation-induced transition between states that are in either equilibrium or far from equilibrium. For equilibrium systems, after Kramers' seminal work [1], many theories have been suggested [2] and tested in many different experiments, which, for example, included optically trapped Brownian particles [3,4], analog circuits [5], and semiconductor lasers [6]. Recently, there have been several experiments concerning systems far from equilibrium, such as the Penning trap [7], vibration-fluidized granular matter [8], and Josephson junction [9]. Theoretical works were performed on the calculation of the transition rates [10,11] or the transition paths [12]. These theories showed the transitions in many systems far from equilibrium could be described by the Kramers' equation in equilibrium. However, except for the Penning trap, the only quantitatively investigated experimental system was the analogue electrical circuit [13], which can be considered as analogue simulations. For the Penning trap, on the other hand, the experiment was carried out within a very narrow parameter region; only near the bifurcation points.

In this paper, we report on the experimental study of noise-induced transition in the parametrically excited magneto-optical trap (MOT) which is a system far from equilibrium. We show that the equilibrium theory of the fluctuation-induced transition can be quantitatively applied to the driven atomic system far from equilibrium. In particular, we have investigated experimentally the transitions in nearly full parameter regions from super-critical bifurcation points (dynamic double attractors) to subcritical bifurcation points (dynamic triple attractors). For double attractors, we measured the transition rates by directly observing the change of population difference between two oscillating wells at various modulation frequencies and modulation amplitudes. The transition between three attractors, on the other hand, which to our knowledge has never been investigated experimentally, was studied indirectly by measuring the populations in each well.

For the two attractors, the experimentally measured transition rates were found in quantitative agreement with the theoretical values and Monte Carlo simulation results. The theory of transition far from equilibrium can be called a dynamic version of Kramers' equation, which was obtained by changing the transitions between dynamic states to those between static wells in phase-space Hamiltonian through averaging method. The simulations were based on the Langevin equations, which describe well the quantum dissipation [14] including spontaneous emissions, the origin of fluctuations of atomic motion in MOT. For the three attractors, the experiments were also in agreement with simulations, and showed qualitatively the same dependence on the modulation frequency. In the quantitative point of view, however, the phase-space Hamiltonian approach suffered from some disagreement with the experiments. We will discuss the limit of the Hamiltonian method to study the transitions among three attractors at the end of the paper.

As reported in previous papers [15], our experiments were well described by the simple Doppler theory of MOT, which can be expanded to the third order and written by

$$\ddot{z}+\beta\dot{z}+\omega_0^2(1+h\cos\omega t)z=-A_0\omega_0^2\left[z+\frac{\hbar k}{\mu_B b}\dot{z}\right]^3, \quad (1)$$

where the natural trap frequency of MOT is $\omega_0=2\pi f_0=\sqrt{8k\mu_B b s_0\delta/[m(1+4\delta^2)^2]}$, the damping coefficient is $\beta=(\hbar k/\mu_B b)\omega_0^2$, and the coefficient of third order term is $A_0=8(\mu_B b/\hbar\Gamma)^2(4\delta^2-1)/(4\delta^2+1)^2$. Here m is the mass of an atom, k is the wave vector, Γ is the decay rate of the excited state, $\delta=-\Delta/\Gamma$ is the normalized frequency detuning for the laser detuning of Δ, $s_0=I/I_s$ is the normalized laser intensity I with respect to the saturation intensity I_s, μ_B is the Bohr magneton, b is the magnetic field gradient, h is the modulation amplitude, and $\omega=2\pi f$ is the modulation angular frequency.

When the intensity-modulation frequency f of the cooling laser is around twice the trap frequency between f_1 and f_2,

*Present address: Institute for Experimental Physics, University of Innsbruck, 6020 Innsbruck, Austria
†Corresponding author: whjhe@snu.ac.kr

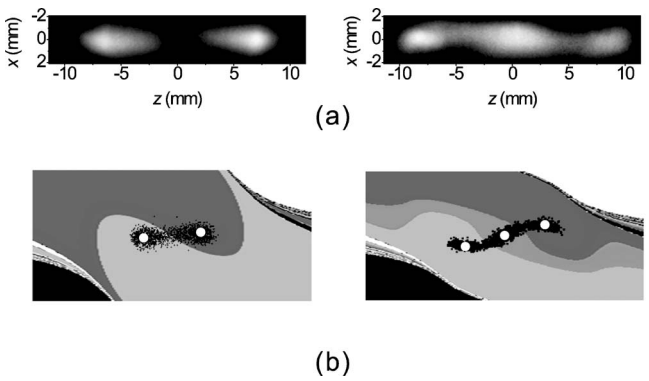

FIG. 1. (a) The atomic fluorescent images of the LC motion in the position space for two attractors (left) and three attractors (right). The abscissas and ordinates are in unit of mm. (b) A phase-space map for two (left) and three (right) attractor conditions, where square dots in each basin represent the phase-space attractors. The horizontal side of the rectangle-shaped maps represents the position from −20 mm (left end) to +20 mm (right end), whereas the vertical side indicates the velocity from −4.85 m/s (bottom) to +4.85 m/s (top) for the left figure and that from −6.6 m/s (bottom) to +6.6 m/s (top) for the right one.

atoms are separated into two clouds [Fig. 1(a), left] and oscillate in out-of-phase motion, which corresponds to the limit-cycle (LC) characterized by dynamic double attractors. Due to the nonlinearity associated with MOT, as f is increased above f_2 but below f_3, an additional stable attractor appears at the center of the LC motion, which is called subcritical bifurcation [Fig. 1(a), right]. Given the modulation amplitude h, the corresponding frequencies are, $f_1=2f_0-(f_0/2)\sqrt{h^2-h_T^2}$, $f_2=2f_0+(f_0/2)\sqrt{h^2-h_T^2}$, and $f_3=f_0+(hf_0/2h_T)\sqrt{4+h_T^2}$, where $h_T=\beta/(\pi f_0)$ is the threshold value of h for the parametric resonance to occur for a given β.

Assuming no fluctuations in atomic motion, the initial conditions of atomic position and velocity determine which attractors (represented by square dots) an atom ends up with. Figure 1(b) shows each region of two attractors (left) and that of three attractors (right). For example, if the initial condition of an atom lies in the light gray region, the atom approaches the attractor located in the same basin. In reality, however, atomic fluctuating motions exist due to spontaneous emission resulting in broadened distributions of atomic position and velocity near the stable attractors. For large diffusion of atomic motion due to spontaneous emissions, certain atoms may jump far from the original attractor and be transferred to another attractor through the unstable regions near the boundary. In this case, the shape of the atomic phase-space distribution resembles a dumbbell which has a narrow neck near the unstable point. Note that the distribution in Fig. 1(b) represents the shape of dynamic potential well, as discussed in the static potential situation [4].

The transitions between the dynamic attractors can be well described by the transitions between the static potential wells, because the dynamic attractor can be interpreted as a potential well in phase-space Hamiltonian. After transforming to the rotating frame with the same frequency of the modulation, we obtain a Hamiltonian-like function in phase space. We change variables $z=x\cos(\omega t/2)-y\sin(\omega t/2)$, $\dot{z}=-\omega/2[x\sin(\omega t/2)+y\cos(\omega t/2)]$ in Eq. (1), apply the method of averaging, ignore the dissipation terms, and find the Hamiltonian-like function from the Hamiltonian equations of x and y variables [11]. The Hamiltonian exhibits the double-well feature for the parameters of two attractors, whereas it shows the triple-well structure for those of three attractors.

In real-space potential and equilibrium, it is well known that the Kramers' escape rate is written by $\exp(-\Delta U/k_BT)$, where ΔU is the potential depth and k_BT is the amount of fluctuations from thermal energy. With the use of the Hamiltonian-like function, the escape rate in phase space can be written by $W\propto\exp(-S/D)$, which is the dynamic version of the Kramers' equation. Here S and D are the activation energy and the amount of diffusion in phase space that is proportional to the diffusion constant of MOT, which correspond to ΔU and k_BT in the Kramers' formula, respectively. As observed in the stationary position-space potentials, the escape rate increases as the diffusion increases or the activation energy decreases.

When $f_1<f<f_2$, since there are only two dynamic wells, the escape from one well means the transition to the other well. Since all the nonlinear terms in the equations of motion of MOT have the same sign as the first order term, the activation energy is proportional to f and h. Due to symmetry between the two wells, the transition rate from state 1 to 2 is the same as that from state 2 to state 1. Around the supercritical bifurcation point (i.e., the starting point for two attractors), one can find that the transition rates approximately vary as,

$$W=c_1\exp\left[-\frac{c_2}{hD}(f-f_1)^2\right], \tag{2}$$

where f_1 is the modulation frequency at the bifurcation point and c_1 and c_2 are constants [10]. The constant $c_2=(1/f_0^2)\sqrt{2/h_T}$ was obtained by direct calculation of activation energy S_n $(n=1, 2)$. The diffusion coefficient D in phase space is closely related to the Doppler diffusion (DD) coefficient of MOT by the equation $D=3A_0/(2m^2\omega_0\beta^2)$ DD [10]. Since usually DD is very difficult to obtain by simple calculation from experimental parameters, we have used D as fitting parameter with the constant c_1. Note that one can directly measure the quantity of Eq. (2) by removing one state population and observing the recovering process.

When $f_2<f<f_3$, the same calculations of activation energy can be performed but the aspects of transitions become rather complicated. The phase space potential shows that transition occurs only between one of the two dynamic states (state 1 or state 2) and the stable state (state 0), with no possibility of direct transitions from 1 to 2 or 2 to 1. Unlike the double-well case, the transition rates W_{i0} from state i to 0 are not necessarily the same as W_{0i} from state 0 to i $(i=1, 2)$. In experiments, due to technical reasons to be described later, we have studied the transitions in the subcritical region by using an indirect method of measuring the populations in each state.

The ratios of the population N_1 or N_2 to N_0 can be used to obtain the ratio of the transition rates, that is, N_1/N_0

$=N_2/N_0=W_0/2W$, where we have employed $W_{10}=W_{20}=W$ and $W_{01}=W_{02}=W_0/2$. The theoretical calculation is written by $W_0/W=\exp[(S_1-S_0)/D]$ and S_n is obtained from the Hamiltonian function [10]. For the triple attractors, the S_n can be calculated not analytically but numerically. Qualitatively the activation energy of state 0 increases while the energy of state 1 and 2 decreases as f increases. In our experiments, for larger modulation frequency, N_0 becomes larger than N_1 and N_2, which means W_0/W becomes smaller as expected.

Unlike the single electron in the Penning trap, there are more than 10^7 atoms in the initial MOT and each cloud of the LC motion under parametric excitation is almost equally populated. In order to monitor the transition between two dynamic attractors, one of the clouds needs to be blown away by using a resonant laser because the number of atoms transferred from attractor 1 to 2 is the same as that from 2 to 1. When atoms, say in attractor 1, are removed, one can observe that some atoms in attractor 2 are transferred to 1 with the passage of time. Due to the two-way transitions the population difference decreases exponentially. For many particle systems the transitions can be described by the following simple rate equations:

$$\frac{dN_1}{dt} = R - \gamma N_1 - W_1 N_1 + W_2 N_2,$$

$$\frac{dN_2}{dt} = R - \gamma N_2 - W_2 N_2 + W_1 N_1, \tag{3}$$

where N_1 and N_2 are the populations of the attractors one and two, respectively, R is the trap loading rate, γ is the loss rate due to collisions by the background atoms, and $W_1(W_2)$ is the transition rate from the attractor 1 to 2 (2 to 1). Since R and γ are small in our experiment as discussed later, we neglect these terms and also assume $W=W_1=W_2$ due to the symmetry. Thus the steady-state solution of the population difference $\Delta N=N_2-N_1$ is given by

$$\Delta N = \Delta N_0 e^{-2Wt}, \tag{4}$$

where ΔN_0 is the difference right after atoms in one cloud is blown away.

Our experimental setup is similar to that described in our previous work [15] but with new added features; we used a photodiode array [16] to measure the transition rates and used a resonant laser to selectively blow away one atomic cloud (say, $n=1$). The blowing laser was cylindrically focused at 5 mm left from the center of the LC motion. The intensity of the laser was over five times the saturation intensity and the laser was turned on for 3 ms in order to remove only one atomic cloud.

Experimental results for double (triple) attractors were obtained at the intensity of $0.034\ I_s(0.06I_s)$ and the detuning of -2.7Γ for the cooling laser along the longitudinal z axis, and the magnetic field gradient of 10 G/cm, where $I_s=3.78\ \mathrm{mW/cm^2}$ is the averaged saturation intensity and $\Gamma=2\pi\times 5.9$ MHz is the natural linewidth. The laser intensity and detuning along the transverse x and y axis are $0.63I_s$ and -3.0Γ, respectively. For these parameters, the measured trap

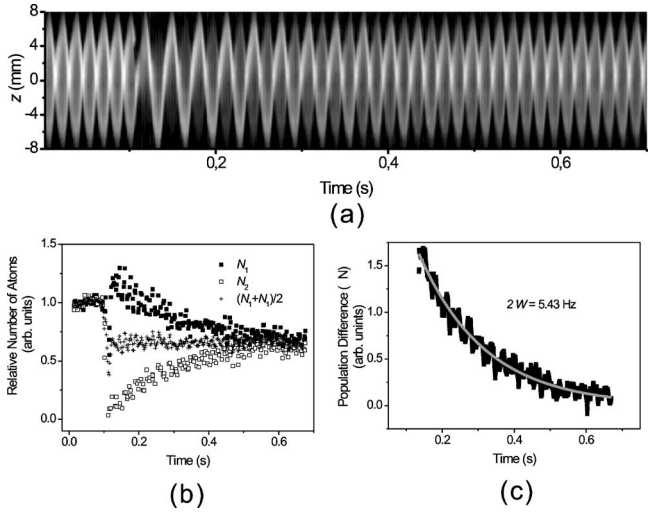

FIG. 2. (a) A typical contour plot of absorption signals obtained at $f=63$ Hz$(f/f_0=1.9)$ and $h=0.7$. (b) Decay of the population of state 2 (filled box), growth of the atomic number of the empty state 1 (empty box) as measured from (a), and the average of the total number (cross). (c) The population difference between the two states shows an exponential decay.

frequency is 33.4 ± 0.5 Hz (43.9 ± 0.8 Hz, for triple states), and the detected damping coefficient is $45.4\pm1.5\ \mathrm{s^{-1}}$ (for triple states, $85.9\pm3.6\ \mathrm{s^{-1}}$), which are in agreement with the simple Doppler theory. Note that the sub-Doppler feature of MOT is dramatically suppressed when the transverse laser detuning is slightly different from that of the z-axis laser [see Fig. 1(a)]. In this situation, the damping coefficient in the z-direction is much reduced, which results in great reduction of the sub-Doppler feature, as discussed in depth in our previous works [16].

The typical data concerning the transition between dynamic double wells are presented in Fig. 2. Figure 2(a) shows a contour plot generated by the atomic absorption signals recorded on the 16 channel photodiode array. The vertical axis represents the atomic position and the longitudinal axis the time evolution. In Fig. 2(a), a large absorption or a large atomic number is indicated by a bright color. From Fig. 2(a) one can trace the oscillating LC attractors and measure the atomic number. One attractor is made empty by using a blowing-up laser at seven half cycles from the left, and then repopulated with time evolution, as plotted in Fig. 2(b). Figure 2(b) is acquired from the amount of absorption of each channel. Figure 2(c), obtained from Fig. 2(b), shows the temporal variation of the population difference ΔN, which clearly shows the exponential decay as expected in Eq. (4) where the decay rate is twice the transition rate. Note that the total number of atoms is nearly all conserved during the transitions [crosses in Fig. 2(b)], which justifies the neglect of the loading rate R and loss rate γ in Eq. (3). In reality, the loss rate of our MOT is $0.15\ \mathrm{s^{-1}}$ which is much smaller than the typical transition rates.

The experimental results in Fig. 3 shows the transition rate dependence on (a) the various modulation frequencies at $h=0.72$ and (b) on the modulation amplitudes at $f/f_0=1.89$. Each point in Fig. 3 was obtained by exponential fitting of

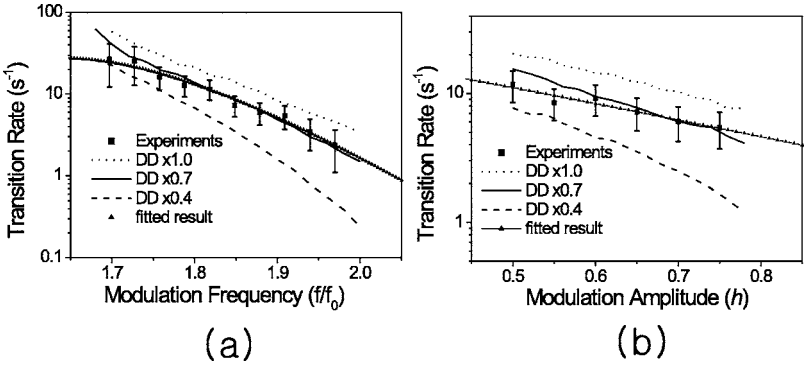

FIG. 3. The transition rates for various (a) modulation frequencies and (b) modulation amplitudes, compared with the Monte Carlo simulations for scaled diffusion D.

Fig. 2(c) and the error bar was the standard deviation of ten experiments. We have compared the experiments to the Monte Carlo simulations. The solid, dotted, and dashed curves in Fig. 3 represent the simulation results from different diffusions. As seen in Fig. 3, the experimental results are in agreement with the simulations when diffusion constant is 0.7 times DD calculated with the simple Doppler theory. We executed the simulations with the simple Doppler equation based on two-level atoms and have included random spontaneous emissions emitted at the rate given by Doppler theory. We first calculated the trajectories of atomic motion of 10^4 atoms initially in $n=2$ state and monitored the subsequent time evolution of the population of the two states. We have then obtained the transition rates by fitting Eq. (4). We also fitted the experimental results with Eq. (2), which is represented by the triangles in Fig. 3(a). Even though the calculations are mainly well applied in the limit $f \gtrsim f_1$ and $\beta \ll \omega_0$, one can see these fittings well describe the experimental results. The consequent diffusion D after fitting is 0.071(±0.008), which is of similar value to the calculated value.

The experimental and simulation results of dynamic triple attractors are shown in Fig. 4. For the case of dynamic triple attractors we indirectly studied the transition rates; we measured the population of each state and observed the dependence of population ratio $(N_1+N_2)/N_0$ on the experimental parameters. The reason why we used this indirect method was that the transition rates were comparable to the loading rates when $f > f_2$ in the actual experiment. It was thus very difficult to distinguish the real transitions and the loading effects after atoms were blown off. Figure 4(a) shows the motions of atomic clouds during single period of oscillation, which provides the population in each state. States one and two show out-of-phase oscillating motions, while state zero remains at the center. Our simulations [Fig. 4(b)] have very similar results to the absorption image [Fig. 4(a)], with different spatial resolutions: 1 mm for Fig. 4(a) and 0.1 mm for Fig. 4(b).

Figure 4(c) shows the dependence of the population of each state and the ratio of population on the modulation frequency. In Fig. 4(c), filled triangles (experiment) and solid curves (simulation) are the ratios of N_1+N_2 to N_0, which provides the ratio of the transitions rates W_0/W. One can observe the ratio of population is decreased as f increases, which means that the transition rate W_0 decreases while W increases. The trend is in qualitative agreement with theoretical expectations, and the simulations reproduce the experimental results very similarly. The data of $(N_1+N_2)/N_T$ (filled boxes) and N_0/N_T (filled circles) in Fig. 4(c) were obtained by fitting the profiles of Fig. 4(a) at 0.58π phase. The dashed curves $(N_1+N_2)/N_T$ and dotted curves N_0/N_T are derived from Fig. 4(b) at 0.5π. Here N_n ($n=0$, 1, 2) is the population of the state n and $N_T=N_0+N_1+N_2$. The profile at that phase shows three peaks, representing three states, are fitted by triple Gaussian functions.

For the subcritical region, experimental results were not in quantitative agreement with the values calculated from the phase-space Hamiltonian theory. The primary difference was associated with f_3, which is the marginal frequency of subcritical bifurcation. In the above given experimental parameters, f_3 was $2.5f_0$ both in the experiments and the simulations, whereas f_3 was larger than $10f_0$ in the phase-space Hamiltonian approach. There was also disagreement between the calculated frequency of $4f_0$ when $W_0/W > 0.5$ and the measured frequency of $2.4f_0$. We think the main reason of these discrepancies between the phase-space Hamiltonian calculations and the experiments is that the calculations are mainly well applied in the limit $\omega - 2\omega_0 \ll \omega_0$ and we have

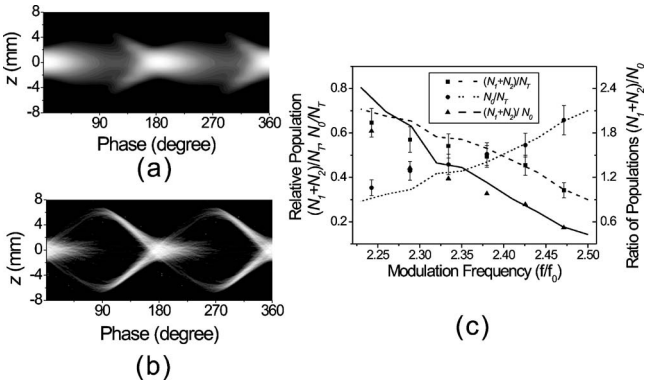

FIG. 4. (a) A contour plot of the absorption signals for triple well conditions, where $f=106$ Hz$(=2.42f_0)$ and $h=0.72$. (b) The contour plot of the simulation results, where $f=105.3$ Hz$(=2.41f_0)$ and $h=0.7$. In (a) and (b), the scale of the vertical axis is ±8 mm and the horizontal axis represents two oscillation periods. (c) The relative populations of states 1 and 2 $(N_1+N_2)/N_T$ compared to that of state 0, N_0/N_T, where points (filled box and filled circle) represent the experimental results and curves the simulations. Filled triangles show the experimental ratios of N_1+N_2 to N_0 and curves the simulation results.

neglected the dissipation effect when we derive the Hamiltonian. In other words, the dissipation shrinks the value of f_3, which cannot be incorporated in the Hamiltonian approach. It will be therefore needed to develop a theoretical model that describes the transition problem between the attractors in the subcritical bifurcation in terms of the Kramers' theory.

In conclusion, the parametrically driven MOT is an ideal experimental realization of the dynamic double and triple attractors under the conditions far from equilibrium. We have investigated the noise-induced transition at various f and h from the supercritical to the subcritical bifurcation region. The results are well described by the Monte Carlo simulations based on the Langevin equations and the simple Doppler theory. Note that our system may be important and useful to study nonlinear problems associated with transitions in far from equilibrium systems. Moreover, one can develop our system to measure the dependence of the transition rates on the phase of modulation during one period, which has not been explored in experiments [17]. One may also extend our system to the study of transitions between dynamic states due to nonsymmetric oscillations that occur in more nonlinear situations [18].

ACKNOWLEDGMENTS

This work was supported by the Creative Research Initiative of the Korea Ministry of Science and Technology. The research of H. R. Noh was financially supported by a research fund of Chonnam National University in 2004.

[1] H. A. Kramers, Physica (Utrecht) **7**, 284 (1940).
[2] P. Hånggi, P. Talkner, and M. Borkovac, Rev. Mod. Phys. **62**, 251 (1990).
[3] A. Simon and A. Libchaber, Phys. Rev. Lett. **68**, 3375 (1992).
[4] L. I. McCann, M. I. Dykman, and B. Golding, Nature (London) **402**, 785 (1999).
[5] M. I. Dykman, P. V. E. McClintock, V. N. Smelyanski, N. D. Stein, and N. G. Stocks, Phys. Rev. Lett. **68**, 2718 (1992).
[6] J. Hales, A. Zhukov, R. Roy, and M. I. Dykman, Phys. Rev. Lett. **85**, 78 (2000).
[7] L. J. Lapidus, D. Enzer, and G. Gabrielse, Phys. Rev. Lett. **83**, 899 (1999).
[8] G. D'Anna, P. Mayor, A. Barrat, V. Loreto, and F. Norl, Nature (London) **424**, 909 (2003).
[9] N. Grønbech-Jensen, M. G. Castellano, F. Chiarello, M. Cirillo, C. Cosmelli, L. V. Filippenko, R. Russo, and G. Torrioli, Phys. Rev. Lett. **93**, 107002 (2004); I. Siddiqi, R. Vijay, F. Pierre, C. M. Wilson, and L. Frunzio, *ibid.* **94**, 027005 (2005).
[10] M. I. Dykman and M. A. Krivoglaz, Sov. Phys. JETP **50**, 30 (1979).
[11] M. I. Dykman, C. M. Maloney, V. N. Smelyanskiy, and M. Silverstein, Phys. Rev. E **57**, 5202 (1998).
[12] A. D. Ventsel and M. I. Freidlin, Usp. Mat. Nauk **25**, 5 (1970) [Russ. Math. Surveys **25**, 1 (1970)].
[13] D. B. Luchinsky and P. V. E. McClintock, Nature (London) **389**, 463 (1997); D. B. Luchinsky, P. V. E. McClintock, and M. I. Dykman, Rep. Prog. Phys. **51**, 889 (1998).
[14] D. Cohen, Phys. Rev. Lett. **78**, 2878 (1997).
[15] K. Kim, H. -R. Noh, Y. -H. Yeon, and W. Jhe, Phys. Rev. A **68**, 031403 (2003); K. Kim, H. -R. Noh, H. J. Ha, and W. Jhe, *ibid.* **69**, 033406 (2004); K. Kim, H. -R. Noh, and W. Jhe, Opt. Commun. **236**, 349 (2004).
[16] K. Kim, H. -R. Noh, and W. Jhe, Phys. Rev. A **71**, 033413, (2005); K. Kim, K. -H. Lee, M. Heo, H. -R. Noh and W. Jhe, *ibid.* **71**, 053406, (2005).
[17] V. N. Smelyanskiy, M. I. Dykman, and B. Golding, Phys. Rev. Lett. **82**, 3193 (1999).
[18] A. N. Silchenko, S. Beri, D. G. Luchinsky, and P. V. E. McClintock, Phys. Rev. Lett. **91**, 174104 (2003).